DALTON
FULL PAPER

Ruthenium complexes with $N(SPR_2)_2^-$ (R = Ph or Pr^i)

Wa-Hung Leung,*[a] Hegen Zheng,[a,b] Joyce L. C. Chim,[a] Joe Chan,[a] Wing-Tak Wong[c] and Ian D. Williams[a]

[a] *Department of Chemistry, The Hong Kong University of Science and Technology, Clear Water Bay, Kowloon, Hong Kong, PR China. E-mail: chleung@ust.hk*
[b] *Department of Chemistry, Nanjing University, Nanjing, PR China*
[c] *Department of Chemistry, The University of Hong Kong, Pokfulam Road, Hong Kong, PR China*

Received 27th September 1999, Accepted 1st December 1999

Reactions of $[Ru(PPh_3)_3Cl_2]$, $[Ru(CO)_2Cl_2]_x$, or $[Ru(dmso)_4Cl_2]$ (dmso = dimethyl sulfoxide) with KL^R [$L^R = N(SPR_2)_2$, R = Ph or Pr^i] afforded $[Ru(L^R)_2(PPh_3)]$ (R = Ph **1** or Pr^i **2**), *cis*-$[Ru(L^R)_2(CO)_2]$ (L = Ph **3** or Pr^i **4**), or *cis*-$[Ru(L^{Ph})_2(dmso)_2]$ **5**, respectively. The crystal structures of complexes **1** and **2** have been determined. They show weak agostic interaction between Ru and L^R with calculated Ru · · · H–C separations of 3.37 and 2.91 Å, respectively. The Ru–P and average Ru–S distances in **1** are 2.218(1) and 2.400 Å, respectively. The corresponding bond lengths for **2** are 2.210(2) and 2.404 Å. Treatment of **2** with Bu^tNC afforded *trans*-$[Ru(L^{Pr})_2(Bu^tNC)_2]$ **6**, the average Ru–S and Ru–C distances of which are 2.453 and 1.990(3) Å, respectively. Reaction of $RuCl_3$ with KL^R in methanol gave the homoleptic complexes $[Ru(L^R)_3]$ (L = Ph **7** or Pr^i **8**). The average Ru–S distance and S–Ru–S angle in **7** are 2.414 Å and 97.41°, respectively. While complex **1** reacts with pyridine (py) to give $[Ru(L^{Ph})_2(PPh_3)(py)]$ **9**, reaction of **2** with py led to isolation of structurally characterised $[Ru(L^{Pr})_2(SO)]$ **10**. The Ru–S(O) and S–O bond lengths in **10** are 2.0563(11) and 1.447(3) Å, respectively, the Ru–S–O angle being 125.5(2)°. Treatment of **1** with SO_2 afforded structurally characterised *cis*-$[Ru(L^{Ph})_2(PPh_3)(SO_2)]$ **11**. The SO_2 ligand binds to Ru in **11** in a η^1-*S* mode and the Ru–S(O) distance is 2.140(4) Å. Complex **2** reacted with SO_2 to give the μ-sulfato-bridged ruthenium(III) dimer $[\{Ru(L^{Pr})(PPh_3)\}_2(\mu\text{-}SO_4)_2]$ **12**, which has been characterised by X-ray crystallography. The Ru–P and average Ru–S and Ru–O distances in **12** are 2.294(2), 2.321 and 2.133 Å, respectively. Complex **1** is capable of catalysing hydrogenation of styrene in the presence of Et_3N presumably *via* a ruthenium hydride intermediate.

Introduction

Transition metal–sulfur complexes have attracted much attention due to their potential applications to catalytic processes such as hydrodesulfurisation and hydrodenitrification.[1] Of particular interest are Ru–S complexes, which owing to the periodic relationship between Ru and Fe may also serve as functional models for Fe–S proteins.[2] Recently diazene,[3] hydrogen sulfide,[4] nitrido,[5] and hydrido[6] complexes of Ru with sulfur-rich co-ordination spheres have been isolated by Sellmann and co-workers. Dinuclear thiolate-bridged ruthenium complexes have also been demonstrated to catalyse interesting redox reactions[7] and multi-electron transfer processes.[8] In this connection, we become interested in ruthenium complexes with the sterically bulky bis(dialkylthiophosphoryl)amides $N(SPR_2)_2$, which may be viewed as a sulfur analogue of acetylacetonate (acac).

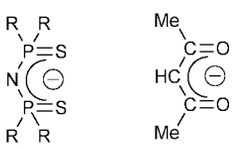

L^R

acac

Unlike acac, L^R ligands exhibit a high degree of geometric and electronic flexibility as they can deviate from planarity without substantial disruption in the P–S π bond. Additionally, the steric and electronic factors of L^R can be tuned easily by the substituents R on phosphorus. Although the co-ordination chemistry of L^R is well documented,[9,10] there are very few examples of their ruthenium complexes.[11] As part of our programme to develop new Ru–S complexes for homogeneous catalysis, we here describe the synthesis and crystal structures of some ruthenium complexes with L^R (R = Ph or Pr^i) and their reactivities toward SO_2 and H_2.

Experimental

All synthetic manipulations were carried out under dry nitrogen by standard Schlenk techniques. Solvents were purified, distilled and degassed prior to use. Infrared spectra (Nujol) were recorded on a Perkin-Elmer 16 PC FT-IR spectrophotometer, mass spectra on a Finnigan TSQ 7000 spectrometer and NMR spectra on a Bruker ALX 300 spectrometer operating at 300 and 121.5 MHz for ^1H and ^{31}P, respectively. Chemical shifts (δ in ppm) were reported with reference to $SiMe_4$ (^1H) and H_3PO_4 (^{31}P). Magnetic moments for solid samples were measured by a Sherwood magnetic susceptibility balance at room temperature. Cyclic voltammetry was performed with a Princeton Applied Research (PAR) Model 273A potentiostat. The working and reference electrodes were glassy carbon and Ag–$AgNO_3$ (0.1 M in acetonitrile), respectively, and the scan rate was 100 mV s^{-1}. Formal potentials ($E°$) were measured in CH_2Cl_2 solutions with 0.1 mol dm^{-3} $[NBu^n_4]PF_6$ as supporting electrolyte and reported with reference to the ferrocenium–ferrocene couple ($Cp_2Fe^{+/0}$). Elemental analyses were performed by Medac Ltd, Surrey, UK.

Materials

The ligands HL^R [$HN(SPR_2)_2$, R = Ph[12] or Pr^i (ref. 13)] were prepared according to the literature methods. The potassium

salts KL^R were obtained by deprotonation of HL^R with 1 equivalent of $K(OBu^t)$ in methanol. The complexes $[Ru(PPh_3)_3Cl_2]$,[14] $[Ru(CO)_2Cl_2]_x$[15] and $[Ru(dmso)_4Cl_2]$ (dmso = dimethyl sulfoxide)[16] were prepared according to the literature methods.

Preparations

$[Ru(L^{Ph})_2(PPh_3)]$ 1. A mixture of $[Ru(PPh_3)_3Cl_2]$ (0.50 g, 0.52 mmol) and 2 equivalents of KL^{Ph} (0.51 g, 1.05 mmol) in tetrahydrofuran (thf) (20 cm^3) was heated at reflux for 3 h. The solvent was pumped off and the residue recrystallised from CH_2Cl_2–Et_2O to give blue crystals (yield 0.50 g, 76%). NMR ($CDCl_3$): ^1H, δ 6.99–7.62 (m, phenyl protons); ^{31}P-{^1H}, δ 37.42 (s, L^{Ph}) and 77.81 (s, PPh_3). $E^\circ = -0.24$ V (Ru^{III}–Ru^{II}) (Found: C, 63.4; H, 4.6; N, 2.2. Calc. for $C_{66}H_{55}N_2P_5RuS_4$: C, 62.9; H, 4.4; N, 2.2%).

$[Ru(L^{Pr})_2(PPh_3)]$ 2. To a solution of $[Ru(PPh_3)_3Cl_2]$ (0.15 g, 0.16 mmol) in thf (20 cm^3) were added 2 equivalents of KL^{Pr} (0.110 g, 0.31 mmol) and the reaction mixture was stirred at room temperature overnight. The solvent was pumped off *in vacuo*, and the residue extracted with hexane. Concentration and cooling at 0 °C afforded air-sensitive blue crystals (yield 0.11 g, 70%). NMR (C_6D_6): ^1H, δ 1.31 (m, 48 H, Me_2CH), 2.21 (m, 8 H, Me_2CH) and 7.14–8.41 (m, 15 H, phenyl H); ^{31}P-{^1H}, δ 60.38 (s, L^{Pr}) and 75.14 (s, PPh_3). MS (FAB): *m*/*z* 988 ($M^+ + 1$). $E^\circ = -0.06$ V (Ru^{III}–Ru^{II}) (Found: C, 49.8, H, 6.7; N, 2.4. Calc. for $C_{42}H_{71}N_2P_5RuS_4\cdot CH_2Cl_2$: C, 48.1; H, 6.8; N, 2.6%).

***cis*-$[Ru(L^{Ph})_2(CO)_2]$ 3.** A mixture of $[Ru(CO)_2Cl_2]_x$ (0.10 g, 0.44 mmol) and 2 equivalents of KL^{Ph} (0.40 g, 0.88 mmol) in dimethylformamide (dmf) (20 cm^3) was heated at reflux overnight. The solvent was distilled off *in vacuo* and the residue extracted with CH_2Cl_2 and purified by column chromatography (neutral alumina). The product was eluted with CH_2Cl_2 as a yellow band. Recrystallisation from CH_2Cl_2–hexane afforded a yellow solid (yield 0.32 g, 69%). NMR ($CDCl_3$): ^1H, δ 7.17–8.14 (m, phenyl H); ^{31}P-{^1H}, δ 39.61 (d, $^2J_{pp} = 4.5$) and 40.41 (d, $^2J_{pp} = 4.5$ Hz). IR (cm^{-1}): 1980 and 2040 [ν(C≡O)]. MS (desorption chemical ionisation, DCI): *m*/*z* 1053 (M^+) (Found: C, 57.3; H, 4.1; N, 2.6. Calc. for $C_{50}H_{40}N_2O_2P_4RuS_4$: C, 57.0; H, 3.8; N, 2.7%).

***cis*-$[Ru(L^{Pr})_2(CO)_2]$ 4.** A mixture of $[Ru(CO)_2Cl_2]_x$ (80 mg, 0.35 mmol) and KL^{Pr} (0.25 g, 0.7 mmol) in dmf (10 cm^3) was heated at 150 °C overnight. The solvent was pumped off and the residue extracted with Et_2O. The product was purified by column chromatography (neutral alumina) using CH_2Cl_2 as eluent. Recrystallisation from hexane at 0 °C afforded a yellow solid (yield 86 mg, 30%). NMR ($CDCl_3$): ^1H, δ 1.18–1.34 (m, 48 H, Me_2CH) and 2.06–2.42 (m, 6 H, Me_2CH); ^{31}P-{^1H}, δ 59.72 (d, $^2J_{PP} = 24.3$) and 61.37 (d, $^2J_{PP} = 24.3$ Hz). IR (cm^{-1}): 1958 and 2023 [ν(C=O)]. MS (FAB): 783 ($M^+ + 1$) and 755 ($M^+ - CO + 1$) (Found: C, 39.8; H, 7.4; N, 3.4. Calc. for $C_{26}H_{56}N_2O_2P_4RuS_4$: C, 39.9; H, 7.2; N, 3.6%).

***cis*-$[Ru(L^{Ph})_2(dmso)_2]$ 5.** To a solution of $[Ru(dmso)_4Cl_2]$ (0.10 g, 0.21 mmol) in thf (20 cm^3) were added 2 equivalents of KL^{Ph} (0.20 g, 0.42 mmol), and the reaction mixture was heated to reflux overnight. The solvent was pumped off *in vacuo* and the residue washed with Et_2O. Recrystallisation from CH_2Cl_2–hexane gave an air-stable yellow solid (yield 0.15 g, 61%). NMR ($CDCl_3$): ^1H, δ 3.07 (s, 6 H, Me_2SO), 3.09 (s, 6 H, Me_2SO) and 7.04–7.89 (m, 40 H, phenyl H); ^{31}P-{^1H}, δ 33.12 (d, $^2J_{pp} = 3.2$) and 34.42 (d, $^2J_{pp} = 3.2$ Hz). IR (cm^{-1}): 1104 [ν(S=O)] (Found: C, 51.2; H, 4.4; N, 2.2. Calc. for $C_{52}H_{52}N_2O_2P_4RuS_6\cdot CH_2Cl_2$: C, 51.4; H, 4.4; N, 2.3%).

***trans*-$[Ru(L^{Pr})_2(Bu^tNC)_2]$ 6.** To a solution of complex **2** (0.1 g, 0.10 mmol) in CH_2Cl_2 (20 cm^3) was added an excess of Bu^tNC (0.05 mL, 0.44 mmol). The reaction mixture was stirred at room temperature for 30 min. The solvent was pumped off *in vacuo*, and the greenish yellow residue washed with hexane. Recrystallisation from CH_2Cl_2–hexane afforded orange crystals (yield: 0.03 g, 34%). NMR ($CDCl_3$): ^1H, δ 1.18–1.28 (m, 48 H, Me_2CH), 1.53 (s br, 18 H, Bu^t) and 2.15 (s br, 8 H, Me_2CH); ^{31}P-{^1H}, δ 60.12 (s). IR (cm^{-1}): 2084 [ν(C≡N)]. $E^\circ = -0.36$ (Ru^{III}–Ru^{II}) and 1.05 V (irrev., Ru^{IV}–Ru^{III}) (Found: C, 45.9; H, 8.5; N, 6.3. Calc. for $C_{34}H_{74}N_4P_4RuS_4$: C, 45.8; H, 8.3; N, 6.3%).

$[Ru(L^{Ph})_3]$ 7. To a solution of $RuCl_3$ (0.1 g, 0.48 mmol) in MeOH (20 cm^3) were added 3 equivalents of KL^{Ph} (0.7 g, 1.44 mmol) and the mixture was refluxed for 2 h. The solvent was pumped off and the residue purified by column chromatography (neutral alumina) using CH_2Cl_2 as eluent. Recrystallisation from MeCN–CH_2Cl_2–hexane afforded blue crystals (yield: 0.21 g, 30%). $\mu_{eff} = 1.7\ \mu_B$. MS (CI): 1446 (M^+) and 998 ($M^+ - L^{Ph}$). $E^\circ = -1.11$ (Ru^{III}–Ru^{II}) and 0.21 V (irrev., Ru^{IV}–Ru^{III}) (Found: C, 59.8; H, 4.2; N, 2.9. Calc. for $C_{60}H_{72}N_3P_6RuS_6$: C, 59.7; H, 4.2; N, 2.7%).

$[Ru(L^{Pr})_3]$ 8. To a solution of $RuCl_3$ (0.1 g, 0.48 mmol) in MeOH (20 cm^3) were added 3 equivalents of KL^{Pr} (0.51 g, 1.44 mmol) and the reaction mixture was heated at reflux in air overnight. Solvent was pumped off and the green residue extracted with hexane and purified by column chromatography (neutral alumina). The product was eluted with acetone–MeOH (1:1) as a blue band. Recrystallisation from hexane afforded a blue crystalline solid (yield: 0.05 g, 10%) (Found: C, 41.4; H, 8.1; N, 4.3. Calc. for $C_{36}H_{84}N_3P_6RuS_6$: C, 41.7; H, 8.1; N, 4.1%).

$[Ru(L^{Ph})_2(PPh_3)(py)]$ 9 (py = pyridine). To a solution of complex **1** (100 mg, 0.08 mmol) was added py (0.05 cm^3) and the mixture stirred at room temperature for 2 h. The solvent was pumped off and the residue washed with hexane. Recrystallisation from CH_2Cl_2–hexane afforded a yellow solid analysed as $[Ru(L^{Ph})_2(PPh_3)(py)]$ in *ca.* 50% yield. NMR spectroscopy indicates that complex **9** in solution is composed of two forms, presumably *cis*- and *trans*-**9**. ^1H NMR ($CDCl_3$): δ 5.18 (t, H_m of py), 6.38 (s br, $H_{m'}$ of py), 6.60–7.81 (m, Ph and H_p of py), 8.31 (d br, H_o of py) and 9.1 (d, $H_{o'}$ of py) (Found: C, 63.4; H, 4.6; N, 2.2. Calc. for $C_{71}H_{60}N_2P_5RuS_4$: C, 62.9; H, 4.4; N, 2.2%).

$[Ru(L^{Pr})_2(SO)]$ 10. To a solution of complex **2** (0.1 g, 0.1 mmol) in hexane (5 cm^3) was added py (0.05 cm^3) and the mixture stirred overnight. Evaporation of the solvent afforded a brown residue, which on recrystallisation from Et_2O–hexane yielded **10** (15 mg, 20%) along with an unidentified brown solid (yield: 15 mg). NMR ($CDCl_3$): ^1H, δ 1.16–1.33 (m, 48 H, CH_3) and 2.13–2.44 (overlapping q, CH); ^{31}P, δ 59.17 (s). IR (cm^{-1}): 1106 [ν(SO)].

***cis*-$[Ru(L^{Ph})_2(PPh_3)(SO_2)]$ 11.** A solution of complex **1** (50 mg, 0.04 mmol) in CH_2Cl_2 (10 cm^3) was bubbled with SO_2(g) for 2 min. The solvent was pumped off and the residue recrystallised from CH_2Cl_2–hexane to give yellow crystals (30 mg, 50%). NMR ($CDCl_3$): ^1H, δ 6.90–8.35 (m, phenyl protons); ^{31}P, δ 27.04, 35.08, 36.52, 42.52 and 43.10 (all ill resolved multiplets). IR (cm^{-1}): 1286 [ν(S=O)] (Found: C, 56.7; H, 3.9; N, 2.0. Calc. for $C_{66}H_{55}N_2O_2P_5RuS_5\cdot CH_2Cl_2$: C, 57.1; H, 4.0; N, 2.0%).

$[\{Ru(L^{Pr})(PPh_3)\}_2(\mu\text{-}SO_4)_2]$ 12. A solution of complex **2** (0.1 g, 0.1 mmol) in CH_2Cl_2 (15 cm^3) was bubbled with SO_2(g) for 2 min. The solvent was pumped off and the residue recrystallised from CH_2Cl_2–hexane to give green crystals (yield 55 mg, 71%). IR (cm^{-1}): 1130 [ν(SO)]. $\mu_{eff} = 1.7\ \mu_B$ per Ru (Found: C, 45.6; H, 5.7; N, 1.8. Calc. for $C_{68}H_{86}N_2O_8P_6Ru_2S_6\cdot CH_2Cl_2$: C, 45.0; H, 5.4; N, 1.7%).

Catalytic hydrogenation of styrene with complex 1

A mixture of complex **1** (0.080 g, 0.06 mmol) and styrene (0.066 g, 0.60 mmol) was stirred in thf (10 cm^3) in the presence of Et_3N (0.05 cm^3) under hydrogen (1 atm) at room temperature overnight. The organic product was characterised as ethylbenzene by GLC and quantified by the internal standard method. The yield of ethylbenzene was determined to be *ca.* 90% with respect to styrene used.

X-Ray crystallography

Pertinent crystallographic data and other experimental details for complexes **1**, **2**, **6**, **7**, and **10**–**12** are summarised in Table 1. Data were collected on a MAR research image diffractometer (for **1**, **2**, **7** and **12**), a Rigaku AFC7R (for **11**), and a Siemens P4 diffractometer (for **6** and **10**) using Mo-Kα radiation (λ = 0.71073 Å) with a graphite crystal monochromator in the incident beam. The diffracted intensities were corrected for Lorentz-polarisation effects. An approximate absorption correction by interimage scaling was applied for complexes **1**, **2**, **7** and **12**. All the structures were solved by direct methods and expanded by Fourier-difference techniques. Except for complex **10**, which was refined on F^2, they were refined on F. For **2**, a restraint on the C–C distance of the isopropyl groups of L^{Pr} of 1.54 Å was included in the refinement. For **7** a positional disorder problem associated with one of the phenyl rings in L^{Ph} [C(62)–C(63)–C(64)–C(65)–C(66)–C(67)] was encountered. A model with two sites for the phenyl ring with occupancies of 0.5 each was used for refinement; hydrogen atoms of this disordered phenyl ring were not included. Structure **10** was refined with the disordered isopropyl carbon C(41) split into two sites of 0.6 and 0.4 occupancy, with each refined isotropically. The carbon atom C(40) also shows signs of disorder and has somewhat enlarged thermal parameters U_{11}, but was refined anisotropically. The bond lengths from C(40) had restraints applied, though both C(40)–C(41) and C(40)–C(41a) still show shortening (1.38 Å) due to librational motion of C(40). For complex **11** the carbon atoms of the disordered phenyl ring were refined with restraints on C–C distances (1.44 Å) and C–C–C angles (120°). Site occupancies of 0.5 each were used for refinement. Calculations were performed on a Silicon-Graphics computer, using the program packages TEXSAN[17] (for **1**, **2**, **7**, **11** and **12**) and SHELXL[18] (for **6** and **10**). Selected bond lengths and angles for **1**, **2**, **6**, **7**, **10**–**12** are listed in Tables 2–8, respectively.

CCDC reference number 186/1751.

See http://www.rsc.org/suppdata/dt/a9/a907753g/ for crystallographic files in .cif format.

Results and discussion

Ruthenium(II) complexes with L^R (R = Ph or Pr^i)

The syntheses of Ru–L^R complexes (R = Ph or Pr^i) are summarised in Scheme 1. Interaction of $[Ru(PPh_3)_3Cl_2]$ with KL^R in thf afforded $[Ru(L^R)_2(PPh_3)]$ (R = Ph **1** or Pr^i **2**) isolated as bluish green crystals. Complex **1** is stable in the solid state but readily air oxidised in solution to give a paramagnetic green species, presumably a ruthenium(III) complex. Complex **2** was found to be air sensitive in both the solid state and solution. The solid-state structures of **1** and **2** have been determined and are shown in Figs. 1 and 2, respectively. The corresponding selected bond lengths and angles are listed in Tables 2 and 3. The geometry around Ru in both complexes is pseudo square pyramidal with four sulfurs at the square base and PPh_3 at the apical position. This geometry is in contrast with that of the related Sellmann Ru^{II}–'S_4' type compounds ('S_4'$^{2-}$ = 1,2-bis(2-sulfanylphenyl)-sulfanyl)ethanide(2−)),[3,4,6] which are octahedral, indicative of the steric bulk of the L^R ligands. The Ru–P and average Ru–S distances in **1** (2.218(1) and 2.400 Å) and **2** (2.210(2) and 2.404 Å) are similar to those in $[\{Ru(PPh_3)('^{bu}S_4')\}_2(\mu\text{-}N_2H_2)]$ ('$^{bu}S_4$'$^{2-}$ = 1,2-bis(3,5-di-*tert*-butyl-2-sulfanylphenyl)sulfanyl)-ethanide(2−); 2.232(3) and 2.357 Å, respectively).[2] The average S–Ru–P angles in **1** and **2** are 97.18 and 97.53°, respectively. For **1**, one phenyl ring of L^{Ph} is found to bend toward Ru, suggestive

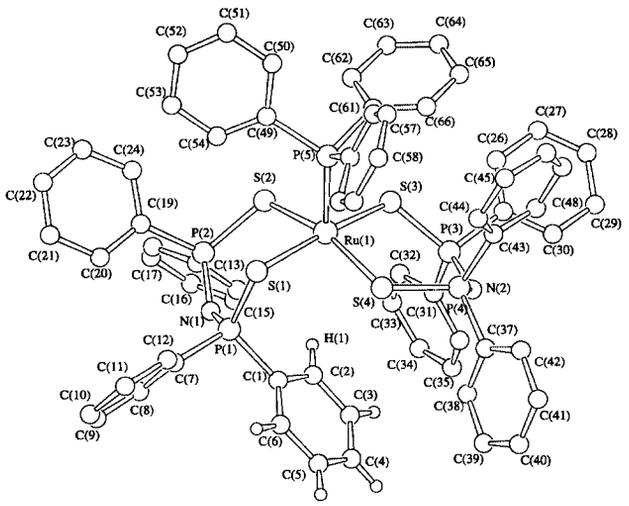

Fig. 1 Perspective view of $[Ru(L^{Ph})_2(PPh_3)]$ **1**.

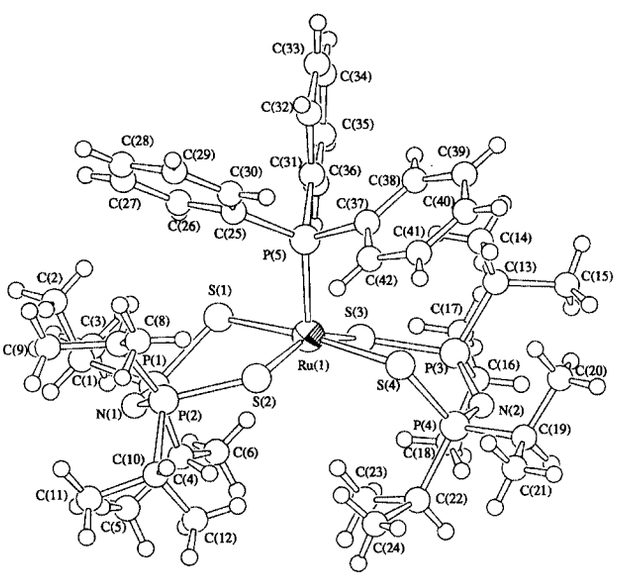

Fig. 2 Perspective view of $[Ru(L^{Pr})_2(PPh_3)]$ **2**.

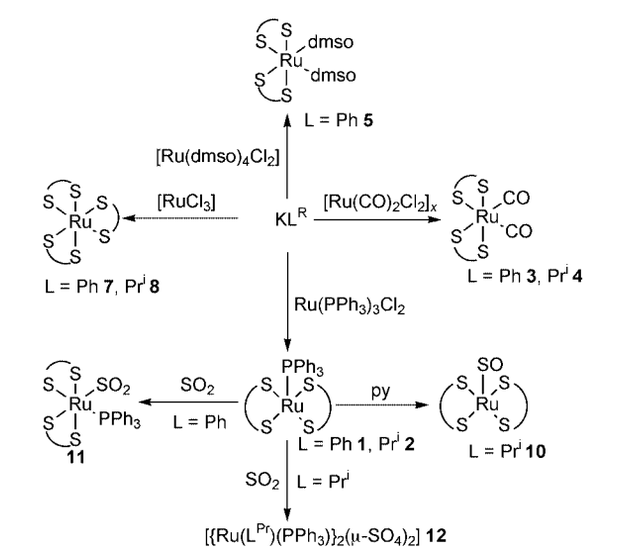

Scheme 1

Table 1 Crystallographic data and experimental details for $[Ru(L^{Ph})_2(PPh_3)]\cdot CH_2Cl_2$ **1**·CH_2Cl_2, $[Ru(L^{Pr})_2(PPh_3)]$ **2**, *trans*-$[Ru(L^{Pr})_2(Bu^tNC)_2]$ **6**, $[Ru(L^{Ph})_3]\cdot\frac{1}{2}$MeCN **7**·$\frac{1}{2}$MeCN, $[Ru(L^{Pr})_2(SO)]$ **10**, *cis*-$[Ru(L^{Ph})_2(PPh_3)(SO_2)]\cdot CH_2Cl_2$ **11**·CH_2Cl_2, and $[\{Ru(L^{Pr})(PPh_3)\}_2(\mu\text{-}SO_4)_2]$ **12**

	1·CH_2Cl_2	**2**	**6**	**7**·$\frac{1}{2}$MeCN	**10**	**11**·CH_2Cl_2	**12**
Empirical formula	$C_{66}H_{55}N_2P_5RuS_4$	$C_{42}H_{71}N_2P_5RuS_4$	$C_{34}H_{74}N_4P_4RuS_4$	$C_{61.5}H_{73}N_{3.5}P_6RuS_6$	$C_{24}H_{56}N_2OP_4RuS_5$	$C_{67}H_{57}Cl_2N_2O_2P_5RuS_5$	$C_{34}H_{43}NO_4P_3RuS_3$
M	1260.35	988.22	892.2	1467.09	774.0	1409.34	771.85
Crystal system	Triclinic	Triclinic	Monoclinic	Monoclinic	Monoclinic	Triclinic	Monoclinic
Space group	$P\bar{1}$ (no. 2)	$P\bar{1}$ (no. 2)	$P2_1/c$ (no. 14)	$C2/c$ (no. 15)	$P2_1/n$ (no. 14)	$P\bar{1}$ (no. 2)	$P2_1/a$ (no. 14)
a/Å	11.186(1)	10.142(1)	12.986(2)	47.259(3)	13.920(4)	13.736(5)	13.064(1)
b/Å	12.432(1)	12.570(1)	11.213(2)	11.459(2)	15.486(4)	21.122(5)	17.607(2)
c/Å	21.441(3)	20.791(1)	17.140(3)	26.739(2)	18.123(3)	13.521(6)	15.498(2)
α/°	95.13(2)	81.672(2)				106.91(3)	
β/°	91.70(2)	89.89(2)	105.28(2)	97.98(2)	104.10(2)	117.78(3)	106.29(2)
γ/°	97.48(2)	73.21(2)				88.29(3)	
U/Å^3	2941.9(2)	2508.5(5)	2407.8(7)	14340(2)	3789.8(16)	3294(2)	3421.7(7)
Z	2	2	4	8	2	2	4
D_c/g cm^{-3}	1.423	1.308	1.231	1.359	1.356	1.408	1.498
T/K	298	298	298	298	298	301	298
μ/cm^{-1}	5.88	6.68	6.58	5.71	8.78	6.44	8.17
Reflections collected	15352	8091	5774	8658	9032	9043	6532
observed	6313 ($I > 3.0\sigma(I)$)	6048 ($I > 1.5\sigma(I)$)	4409 ($I > 4.00\sigma(I)$)	4209 ($I > 1.5\sigma(I)$)	8635 ($F > 2.0\sigma(F)$)	3819 ($I > 1.5\sigma(I)$)	4699 ($I > 1.5\sigma(I)$)
R	0.039	0.069	0.0359	0.054	0.0407	0.094	0.059
R′	0.033	0.079	0.0446	0.057	0.087[a]	0.062	0.063

[a] *wR*2 value.

Table 2 Selected bond lengths (Å) and angles (°) for $[Ru(L^{Ph})_2(PPh_3)]$ **1**

Ru(1)–S(1)	2.421(1)	Ru(1)–S(2)	2.415(1)
Ru(1)–S(3)	2.396(1)	Ru(1)–S(4)	2.370(1)
Ru(1)–P(5)	2.218(1)		
S(1)–Ru(1)–S(2)	94.34(4)	S(1)–Ru(1)–S(3)	172.04(4)
S(1)–Ru(1)–S(4)	82.99(3)	S(1)–Ru(1)–P(5)	94.65(4)
S(2)–Ru(1)–S(3)	82.25(4)	S(2)–Ru(1)–S(4)	161.99(4)
S(2)–Ru(1)–P(5)	94.54(4)	S(3)–Ru(1)–S(4)	98.01(4)
S(3)–Ru(1)–P(5)	92.80(4)	S(4)–Ru(1)–P(5)	103.42(4)

Table 3 Selected bond lengths (Å) and angles (°) for $[Ru(L^{Pr})_2(PPh_3)]$ **2**

Ru(1)–S(1)	2.408(2)	Ru(1)–S(2)	2.379(2)
Ru(1)–S(3)	2.403(2)	Ru(1)–S(4)	2.427(2)
Ru(1)–P(5)	2.210(2)		
S(1)–Ru(1)–S(2)	99.67(7)	S(1)–Ru(1)–S(3)	81.09(7)
S(1)–Ru(1)–S(4)	173.57(7)	S(1)–Ru(1)–P(5)	91.37(7)
S(2)–Ru(1)–S(3)	156.13(8)	S(2)–Ru(1)–S(4)	81.52(7)
S(2)–Ru(1)–P(5)	93.60(8)	S(3)–Ru(1)–S(4)	95.25(6)
S(3)–Ru(1)–P(5)	110.26(7)	S(4)–Ru(1)–P(5)	94.87(7)

of an agostic interaction between Ru and the *ortho* C–H of phenyl. Similar Ru···H–C agostic interaction between Ru and a methyl group of L^{Pr} was found for **2**. The calculated Ru···H–C separations for **1** and **2** (3.37 and 2.91 Å, respectively) are, however, longer than those typical for agostic ruthenium(II) phosphine compounds (*e.g.* 2.59 Å for $[Ru(PPh_3)_3Cl_2]$,[19] indicating that the Ru···C–H agostic interactions should be weak. We were not able to detect the agostic hydrogens in **1** and **2** by ^1H NMR or IR spectroscopy. The ^{31}P signal for L^{Ph} in **1** appeared as a singlet at δ 37.42, which is temperature invariant from 25 to −50 °C, suggesting that the L^{Ph} phenyl rings are scrambling rapidly around Ru on the NMR timescale.

Reactions of KL^R with $[Ru(CO)_2Cl_2]_x$ and $[Ru(dmso)_4Cl_2]$ in refluxing dmf afforded *cis*-$[Ru(L^{Ph})_2(CO)_2]$ (R = Ph **3** or Pr^i **4**) and *cis*-$[Ru(L^{Ph})_2(dmso)_2]$ (R = Ph **5**), respectively. Complex **5** could also be prepared by reaction of **1** with dmso. Unlike **1** and **2**, complexes **3**–**5** are air-stable in both the solid state and solution. Consistent with the *cis* geometry, the ^{31}P-$\{^1H\}$ NMR spectra for **3**–**5** show two doublets due to the two non-equivalent phosphorus nuclei in L^R. The $^2J_{PP}$ for **4** (24.3 Hz) was found to be larger than those for **3** and **5** (4.5 and 3.2 Hz). The ν(C≡O) for **4** (1958 and 2023 cm^{-1}) are lower than those for **3** (1980 and 2040 cm^{-1}), indicating that L^{Pr} is a stronger donor than L^{Ph}. The ν(S=O) for **5** of 1104 cm^{-1} is consistent with the *S*-bound mode of the dmso ligands.[20]

Treatment of complex **1** with Bu^tNC afforded a yellow insoluble solid, which has yet to be characterised. Reaction of **2** with Bu^tNC gave *trans*-$[Ru(L^{Pr})_2(Bu^tNC)_2]$ **6**, isolated as an air stable orange solid. The IR spectrum of **6** shows ν(C≡N) at 2084 cm^{-1}, which is lower than that for *trans*-$[Ru(Et_2dtc)_2(Bu^tNC)_2]$ (Et_2dtc = *N*,*N*-diethyldithiocarbamate) (2098 cm^{-1}).[21] The structure of **6** has been established by X-ray crystallography. Fig. 3 shows a perspective view of **6**; selected bond lengths and angles are listed in Table 4. The Ru–C distance of 1.990(3) Å is comparable to that for *trans*-$[Ru(Et_2dtc)_2(Bu^tNC)_2]$ (1.997(2) Å).[21] The average Ru–S distance of 2.453 Å is longer than that in five-co-ordinate **2**.

Table 4 Selected bond lengths (Å) and angles (°) for *trans*-$[Ru(L^{Pr})_2(Bu^tNC)_2]$ **6**

Ru(1)–S(1)	2.456(1)	Ru(1)–S(2)	2.450(1)
Ru(1)–C(1)	1.990(3)	Ru(1)–S(1A)	2.456(1)
Ru(1)–S(2A)	2.450(1)	Ru(1)–C(1A)	1.990(3)
S(1)–Ru(1)–S(2)	99.2(1)	S(1)–Ru(1)–C(1)	82.2(1)
S(2)–Ru(1)–C(1)	97.2(1)	S(1)–Ru(1)–S(1A)	180.0(1)
S(2)–Ru(1)–S(1A)	80.8(1)	C(1)–Ru(1)–S(1A)	97.8(1)
S(1)–Ru(1)–S(2A)	80.8(1)	S(2)–Ru(1)–S(2A)	180.0(1)
C(1)–Ru(1)–S(2A)	82.8(1)	S(1A)–Ru(1)–S(2A)	99.2(1)
S(1)–Ru(1)–C(1A)	97.8(1)	S(2)–Ru(1)–C(1A)	82.8(1)
C(1)–Ru(1)–C(1A)	180.0(1)	S(1A)–Ru(1)–C(1A)	82.2(1)
S(2A)–Ru(1)–C(1A)	97.2(1)		

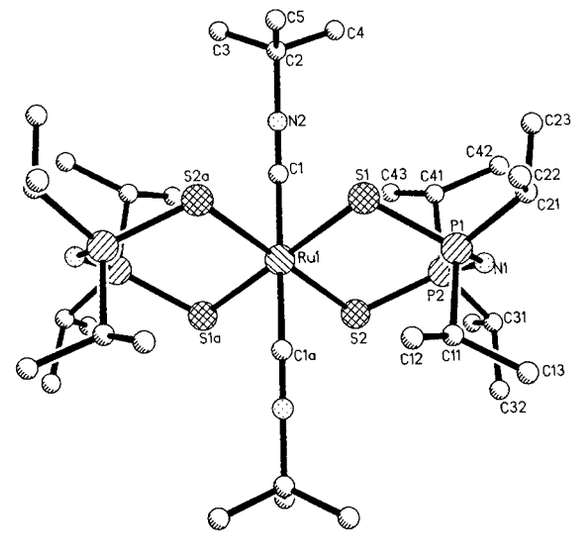

Fig. 3 Perspective view of *trans*-$[Ru(L^{Pr})_2(Bu^tNC)_2]$ **6**.

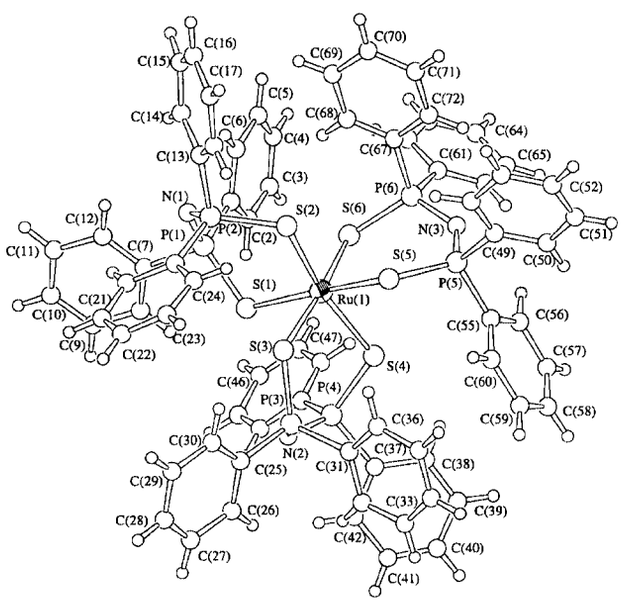

Fig. 4 Perspective view of $[Ru(L^{Ph})_3]$ **7**.

Homoleptic complexes $[Ru(L^R)_3]$

In attempts to prepare higher valent Ru–L^{Ph} complexes, reactions of oxo- and nitrido-ruthenium(VI) complexes with KL^{Ph} were studied. Treatment of $[RuO_2Cl_3]^-$ [22] with KL^{Ph} resulted in a dark precipitate apparently due to reduction of Ru=O by L^{Ph}. Interaction of $[Ru(N)Cl_4]^-$ [23] with KL^{Ph} in methanol gave the homoleptic complex $[Ru(L^{Ph})_3]$ **7**, which could be prepared directly from $RuCl_3$ and KL^{Ph} in methanol. Complex **7** was presumably formed *via* the reduction of a nitridoruthenium(VI) intermediate because it was found that reaction of $[Os(N)Cl_4]^-$ with KL^{Ph} afforded *trans*-$[Os(N)Cl(L^{Ph})_2]$.[24] Similarly, reaction of $RuCl_3$ with KL^{Pr} in methanol afforded highly soluble $[Ru(L^{Pr})_3]$ **8** in low yield. The measured μ_{eff} of 1.7 μ_B is consistent with a ruthenium(III) formulation for **7**. The solid-state structure of **7** has been confirmed by X-ray crystallography. Fig. 4 shows a perspective view of **7**; selected bond lengths and angles are listed in Table 5. The geometry around Ru is octahedral with the average S–Ru–S angle of 97.41°. The

Table 5 Selected bond lengths (Å) and angles (°) for $[Ru(L^{Ph})_3]$ **7**

Ru(1)–S(1)	2.447(3)	Ru(1)–S(2)	2.377(3)
Ru(1)–S(3)	2.444(3)	Ru(1)–S(4)	2.404(3)
Ru(1)–S(5)	2.438(3)	Ru(1)–S(6)	2.376(3)
S(1)–Ru(1)–S(2)	98.23(10)	S(1)–Ru(1)–S(3)	86.0(1)
S(1)–Ru(1)–S(4)	96.5(1)	S(1)–Ru(1)–S(5)	172.1(1)
S(1)–Ru(1)–S(6)	87.1(1)	S(2)–Ru(1)–S(3)	85.1(1)
S(2)–Ru(1)–S(4)	165.0(1)	S(2)–Ru(1)–S(5)	78.7(1)
S(2)–Ru(1)–S(6)	95.6(1)	S(3)–Ru(1)–S(4)	93.6(1)
S(3)–Ru(1)–S(5)	86.5(1)	S(3)–Ru(1)–S(6)	173.1(1)
S(4)–Ru(1)–S(5)	86.4(1)	S(4)–Ru(1)–S(6)	87.4(1)
S(5)–Ru(1)–S(6)	100.4(1)		

Table 6 Selected bond lengths (Å) and angles (°) for $[Ru(L^{Ph})_2(SO)]$ **10**

Ru(1)–S(10)	2.0563(11)	Ru(1)–S(1)	2.4523(10)
Ru(1)–S(2)	2.3467(9)	Ru(1)–S(3)	2.3383(9)
Ru(1)–S(4)	2.4448(10)	S(10)–O(10)	1.447(3)
S(1)–Ru(1)–S(2)	101.37(3)	S(1)–Ru(1)–S(3)	81.06(4)
S(1)–Ru(1)–S(4)	178.83(3)	S(1)–Ru(1)–S(10)	87.16(4)
S(2)–Ru(1)–S(3)	144.05(4)	S(2)–Ru(1)–S(4)	79.67(3)
S(2)–Ru(1)–S(10)	109.50(4)	S(3)–Ru(1)–S(4)	98.41(4)
S(3)–Ru(1)–S(10)	106.44(4)	S(10)–Ru(1)–S(4)	92.00(4)
Ru(1)–S(10)–O(10)	125.5(2)		

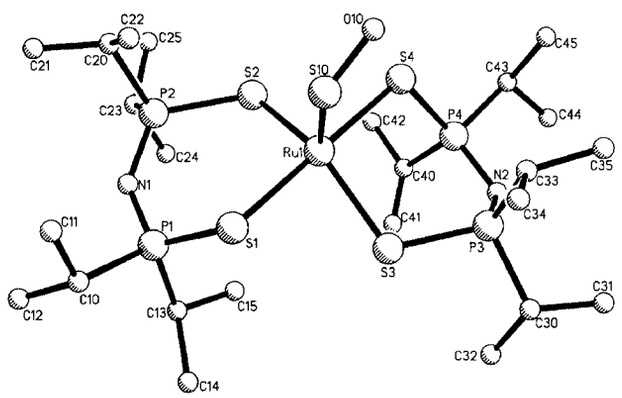

Fig. 5 Perspective view of $[Ru(L^{Pr})_2(SO)]$ **10**.

average Ru–S distance of 2.414 Å is slightly longer than that in **1** possibly due to steric congestion around Ru in the homoleptic complex.

Ruthenium sulfur oxide complexes

As expected co-ordinatively unsaturated complex **1** reacts with Lewis bases to give octahedral adducts. Thus, treatment of **1** with pyridine (py) afforded a yellow solid analysed as $[Ru(L^{Ph})_2(PPh_3)(py)]$ **9**. The ^{1}H NMR spectrum shows two sets of signals due to co-ordinated py, suggesting that **9** in solution is composed of two forms, presumably *cis* and *trans*. We have not been able to separate these two forms by recrystallisation. Interestingly treatment of **2** with py led to isolation of a sulfur monoxide complex $[Ru(L^{Pr})_2(SO)]$ **10** in 20% yield along with an uncharacterised ruthenium product. To our knowledge, complex **10** is the first structurally characterised terminal sulfur monoxide complex of Ru^{II}.[25,26] Fig. 5 shows the molecular structure of **10**; selected bond lengths and angles are listed in Table 6. The geometry around Ru is square pyramidal with the SO ligand occupying the apical position. The average Ru–S(P) distance of 2.3955 Å is similar to that in **2**. The Ru–S(O) and S–O distances (2.0563(11) and 1.447(3) Å, respectively) and Ru–S–O angle of 125.5(2)° in **9** are comparable to those found for $[RuCl(NO)(SO)(PPh_3)_2]$.[25] The IR SO stretching frequency of 1106 cm^{-1} is typical for a terminal SO ligand.[25–27] It seems probable that the extra sulfur in **10** is derived from a free L^{Pr} which is dissociated from **2** upon addition of py. Ruthenium-centred desulfurisation of L^{Pr} afforded a Ru=S intermediate, which was subsequently oxidised by traces of air in the solvent to yield the Ru–SO product **10** (Scheme 2). The fate of the desulfurised L^{Pr}, $[Pr^i_2PNP(S)Pr^i_2]^-$, is not clear. It may be noted that metal-mediated desulfurisation of L^R [28] as well as deoxygenation of co-ordinated SO to give sulfido complexes are well precedented.[10,29]

Table 7 Selected bond lengths (Å) and angles (°) for *cis*-$[Ru(L^{Ph})_2(PPh_3)(SO_2)]$ **11**

Ru(1)–S(1)	2.432(4)	Ru(1)–S(2)	2.421(5)
Ru(1)–S(3)	2.423(5)	Ru(1)–S(4)	2.468(5)
Ru(1)–S(5)	2.140(4)	Ru(1)–P(5)	2.377(5)
S(1)–Ru(1)–S(2)	93.6(2)	S(1)–Ru(1)–S(3)	82.1(2)
S(1)–Ru(1)–S(4)	90.2(2)	S(1)–Ru(1)–S(5)	172.7(2)
S(1)–Ru(1)–P(5)	85.1(2)	S(2)–Ru(1)–S(3)	174.2(2)
S(2)–Ru(1)–S(4)	86.9(2)	S(2)–Ru(1)–S(5)	92.0(2)
S(2)–Ru(1)–P(5)	91.2(2)	S(3)–Ru(1)–S(4)	89.1(2)
S(3)–Ru(1)–S(5)	92.5(2)	S(3)–Ru(1)–P(5)	92.5(2)
S(4)–Ru(1)–S(5)	94.7(2)	S(4)–Ru(1)–P(5)	174.9(2)
S(5)–Ru(1)–P(5)	90.1(2)		

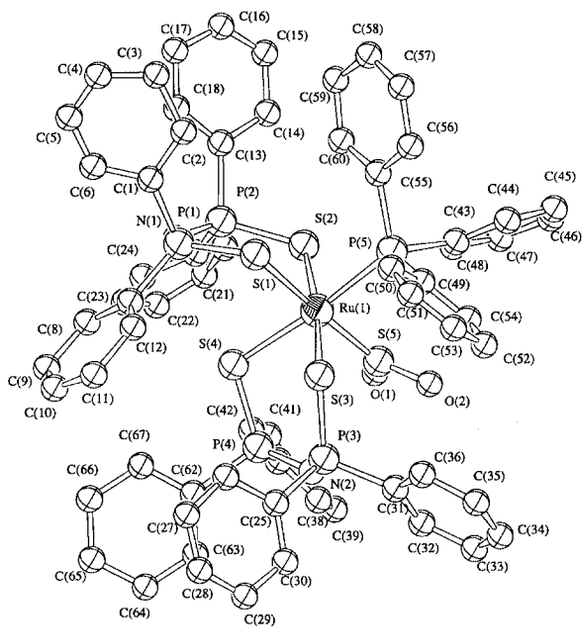

Fig. 6 Perspective view of *cis*-$[Ru(L^{Ph})_2(PPh_3)(SO_2)]$ **11**.

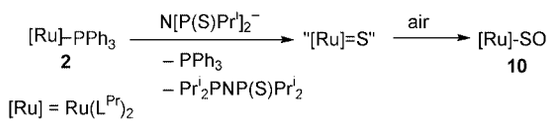

Scheme 2

The observation of high affinity of complex **2** for SO led us to investigate the reactivity of **1** and **2** toward SO_2, which is also a strong π acid. Thus, treatment of **1** with SO_2 gave the expected adduct *cis*-$[Ru(L^{Ph})_2(PPh_3)(SO_2)]$ **11**. The crystal structure of **11** is shown in Fig. 6; selected bond lengths and angles are listed in Table 7. The average Ru–S(P) and Ru–P distances for **11** (2.436 and 2.377(5) Å) are similar to those for **1**. The Ru–S(O) distance of 2.410(4) Å is comparable to that in *trans*-$[Ru(NH_3)_4Cl(SO_2)]^+$.[30] The measured ν(SO) of *ca.* 1286 cm^{-1} is consistent with the *S*-bound, η^1-planar co-ordination mode of SO_2.[31]

On the other hand, reaction of complex **2** with SO_2 yielded a dimeric μ-sulfato-ruthenium(III) complex $[\{Ru(L^{Pr})(PPh_3)\}_2(\mu\text{-}SO_4)_2]$ **12**, which has been unambiguously characterised by X-ray diffraction. The molecular structure is shown in Fig. 7; selected bond lengths and angles are listed in Table 8. The struc-

Table 8 Selected bond lengths (Å) and angles (°) [{Ru(L^{Pr})(PPh_3)}$_2$-(μ-SO_4)$_2$] **12**

Ru(1)–S(2)	2.335(2)	Ru(1)–S(3)	2.307(2)
Ru(1)–P(1)	2.294(2)	Ru(1)–O(1)	2.195(4)
Ru(1)–O(2)	2.063(4)	Ru(1)–O(4)	2.143(4)
S(1)–O(1)	1.499(4)	S(1)–O(2)	1.526(4)
S(1)–O(3)	1.426(4)	S(1)–O(4)	1.462(4)
S(2)–Ru(1)–S(3)	92.86(6)	S(2)–Ru(1)–P(1)	92.97(6)
S(2)–Ru(1)–O(1)	104.2(1)	S(2)–Ru(1)–O(2)	168.4(1)
S(2)–Ru(1)–O(4)	84.5(1)	S(3)–Ru(1)–P(1)	88.49(6)
S(3)–Ru(1)–O(1)	93.2(1)	S(3)–Ru(1)–O(2)	95.2(1)
S(3)–Ru(1)–O(4)	176.7(1)	P(1)–Ru(1)–O(1)	162.6(1)
P(1)–Ru(1)–O(2)	66.9(1)	O(1)–Ru(1)–O(4)	85.9(2)
O(2)–Ru(1)–O(4)	87.3(2)	Ru(1)–O(2)–S(1)	97.8(2)
Ru(1)–O(2)–S(1)	97.8(2)	Ru(1)–O(4)–S(1)	148.8(2)

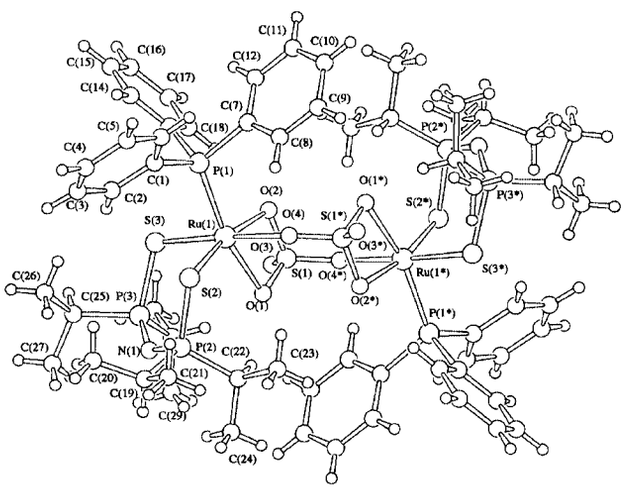

Fig. 7 Perspective view of [{Ru(L^{Pr})(PPh_3)}$_2$(μ-SO_4)$_2$] **12**.

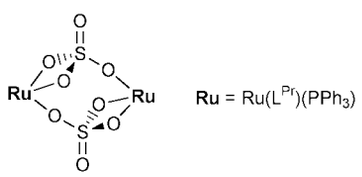

ture consists of two [Ru(L^{Pr})(PPh_3)] moieties, which are bridged by two tridentate μ-κ^1,κ^2-SO_4 dianions. A similar [Ru_2(μ-SO_4)$_2$] core has been observed in [{Ru(PPh_3)$_2$(SO_2)}$_2$(μ-SO_4)$_2$], which was prepared from [Ru(PPh_3)$_4H_2$] and SO_2.[32] The average Ru–S(P) distance (2.321 Å) is shorter than that in **2**. The Ru–P distance for **12** (2.294(2) Å) is longer than that in **2** apparently because Ru^{III} forms a weaker π bond with P than does electron-rich Ru^{II}. The Ru–O bond (2.195(4) Å) that is *trans* to PPh_3 is longer than the other two (2.143 and 2.063 Å), indicative of the *trans* influence of PPh_3. The average Ru–O and S–O distances in **12** are similar to those for [{Ru(PPh_3)$_2$(SO_2)}$_2$(μ-SO_4)$_2$].[32] The measured magnetic moment of 1.7 μ_B per Ru is consistent with the formulation of Ru^{III}. Since the synthesis and purification of **12** was carried out under nitrogen, it seems likely that the oxidation of the co-ordinated SO_2 to SO_4^{2-} is accomplished by disproportionation of SO_2, as in the formation of [Ru(η^5-C_5Me_5)(CO)$_2$(SO_3H)] from [Ru(η^5-C_5Me_5)(CO)$_2$H] and SO_2.[33] The difference in reactivity toward SO_2 between **1** and **2** may be explained by the fact that L^{Pr} is more sterically bulky and thus more labile than L^{Ph}. Pyridine-induced dissociation of L^{Pr} for **2** provides a vacant co-ordination site on Ru for activation and disproportionation of SO_2.

Electrochemistry

Formal potentials of the Ru–L^R complexes have been determined by cyclic voltammetry. The cyclic voltammogram of **1** in CH_2Cl_2 shows a reversible couple at −0.24 V *vs.* $Cp_2Fe^{+/0}$, which is assigned as the metal-centred Ru^{III}–Ru^{II} couple because L^{Ph} is redox inactive at this potential. The Ru^{III}–Ru^{II} potential for **1** is similar to that for *cis*-[Ru(Et_2dtc)$_2$(PPh_3)$_2$] (0.23 V *vs.* standard calomel electrode)[34] and is less cathodic than that for [Et_4N][Ru(N_3)(PCy_3)('S_4')] (Cy = cyclohexyl, −0.26 V *vs.* normal hydrogen electrode).[35] Although the ruthenium(III) state for **1** seems thermodynamically accessible according to cyclic voltammetry, attempts to isolate [Ru^{III}-(L^{Ph})$_2$(PPh_3)]$^+$ by oxidation of **1** with $AgOSO_2CF_3$ or I_2 were unsuccessful. Complex **2** exhibits a reversible Ru^{III}–Ru^{II} couple at −0.06 V, which is less negative than that for **1**. This is quite unexpected given the fact that Pr^i should be more electron-releasing than Ph. It appears that, apart from the electron-releasing ability of L^R, there are other factors affecting the Ru^{III}–Ru^{II} potential for the Ru–L^R complexes. No electro-oxidation was observed for **3** and **5** because the ruthenium(II) state in these complexes is strongly stabilised by back bonding with CO and dmso, respectively. The CV of **6** shows a reversible Ru^{III}–Ru^{II} couple at −0.36 V along with an irreversible oxidation wave at 1.05 V, which is tentatively attributed to Ru^{III}–Ru^{IV} oxidation. The homoleptic complex **7** exhibits reversible couples at 0.21 and −1.11 V, which are assigned as the Ru^{IV}–Ru^{III} and Ru^{III}–Ru^{II} couples, respectively. The reversibility of the Ru^{IV}–Ru^{III} couple for **7** is in contrast to [Ru(Et_2dtc)$_3$], which undergoes irreversible oxidation.[36]

Hydrogenation of styrene catalysed by complex 1

The study of hydrogenation of Ru–S complexes is of interest because it may provide insights into the hydrogen activation mechanism of Fe-only hydrogenases that contain Fe–S clusters in the active sites.[37] Complex **1** was found to catalyse hydrogenation of alkenes in the presence of a base. For example, reaction of styrene with H_2 (1 atm) in the presence of Et_3N and 10 mol% of **1** led to formation of ethylbenzene in over 90% conversion. No hydrogenation was observed when Et_3N was omitted, indicating that the Ru-catalysed hydrogenation proceeded *via* heterolytic cleavage of hydrogen. Heterolytic hydrogen activation by ruthenium complexes with chelating 'S_4' ligand has also been previously reported by Sellmann *et al.*[6] The Ru-containing product isolated from the reaction mixture did not show any ^{31}P resonant signals due to PPh_3, suggesting that PPh_3 dissociation from Ru occurred during catalytic hydrogenation. Attempts to isolate the putative Ru–H intermediate by treatment of **1** with H_2/Et_3N, $NaBH_4$, or Li[BEt_3H] were unsuccessful.

In summary, a series of ruthenium complexes with [$N(PSR_2)_2$]$^-$ have been synthesized and structurally characterised. Co-ordinatively unsaturated [Ru(L^R)$_2$(PPh_3)] were found to have high affinity for sulfur oxide ligands and catalyse hydrogenation of styrene in the presence of Et_3N. The study of other catalytic activities of these electron-rich Ru–S complexes is in active progress.

Acknowledgements

We thank The Croucher Foundation and The Hong Kong University of Science and Technology for support.

References

1 E. I. Stiefel, *ACS Symp. Ser.*, 1996, **653**, 1 and references cited therein.
2 See for example: D. Sellmann and J. Sutter, *Acc. Chem. Res.*, 1997, **30**, 460.
3 D. Sellmann, E. Böhlen, M. Waeber, G. Huttner and L. Zsolani, *Angew. Chem., Int. Ed. Engl.*, 1985, **97**, 984; D. Sellmann and M. Waeber, *Z. Naturforsch., Teil B*, 1986, **41**, 877; D. Sellmann, E. Barth and M. Moll, *Inorg. Chem.*, 1990, **29**, 176; D. Sellmann, J. Käpper, M. Moll and F. Knoch, *Inorg. Chem.*, 1993, **32**, 960.
4 D. Sellmann, P. Lechner, F. Knoch and M. Moll, *J. Am. Chem. Soc.*, 1992, **114**, 922.

5 D. Sellmann and G. Binker, *Z. Naturforsch.*, *Teil B*, 1987, **42**, 341; D. Sellmann, M. W. Wemple, W. Donaubauer and F. W. Heinemann, *Inorg. Chem.*, 1997, **36**, 1397.
6 D. Sellmann, T. Gottschalk-Gaudig and F. W. Heinemann, *Inorg. Chem.*, 1998, **37**, 3982.
7 M. Hidai and Y. Mizobe, *ACS Symp. Ser.*, 1996, **653**, 310 and references cited therein; Y. Nishibayashi, M. Yamanashi, Y. Takagi and M. Hidai, *Chem. Commun.*, 1997, 859.
8 M. Kawano, H. Uemeura, T. Watanabe and K. Matsumoto, *J. Am. Chem. Soc.*, 1993, **115**, 2068.
9 A. Davison and E. S. Switkes, *Inorg. Chem.*, 1971, **10**, 837.
10 J. D. Woollins, *J. Chem. Soc.*, *Dalton Trans.*, 1996, 2893 and references cited therein.
11 A. M. Z. Slawin and J. D. Woollins, *J. Chem. Soc.*, *Dalton Trans.*, 1997, 1877.
12 F. T. Wang, J. Najdzionek, K. L. Leneker, H. Wasserman and D. M. Braitsch, *Synth. Inorg. Metal-Org. Chem.*, 1978, **8**, 120.
13 D. Cupertino, R. Keyte, A. M. Z. Slawin, D. J. Williams and J. D. Woollins, *Inorg. Chem.*, 1996, **35**, 2695.
14 T. A. Stephenson and G. Wilkinson, *Inorg. Nucl. Chem.*, 1966, **28**, 945.
15 F. A. Colton and R. H. Farthing, *Aust. J. Chem.*, 1971, **24**, 903.
16 I. P. Evans, A. Spencer and G. Wilkinson, *J. Chem. Soc.*, *Dalton Trans.*, 1973, 204.
17 TEXSAN, Crystal Structure Package, Molecular Structure Corporation, Houston, TX, 1985 and 1992.
18 SHELXL, G. M. Sheldrick, Siemens Analytical Instruments, Madison, WI, 1993.
19 S. J. LaPlaca and J. A. Ibers, *Inorg. Chem.*, 1965, **4**, 778.
20 K. Nakamoto, *Infrared and Raman Spectra of Inorganic and Coordination Compounds*, 4th edn., Wiley, New York, 1986, p. 268.
21 W.-H. Leung, J. L. C. Chim, H. Hou, T. S. M. Hun, I. D. Williams and W.-T. Wong, *Inorg. Chem.*, 1997, **36**, 4432.
22 S. Perrier and J. K. Kochi, *Inorg. Chem.*, 1988, **27**, 4165.
23 G. W. Griffith and D. Pawson, *J. Chem. Soc.*, *Dalton Trans.*, 1973, 1315.
24 W.-H. Leung, J. L. C. Chim, I. D. Williams and W.-T. Wong, *Inorg. Chem.*, 1999, **38**, 3000.
25 W. A. Schenk and U. Karl, *Z. Naturforsch.*, *Teil B*, 1989, **44**, 998.
26 O. Heyke, G. Beuter and I.-P. Lorenz, *J. Organomet. Chem.*, 1992, **440**, 197.
27 W. A. Schenk, J. Liessner and C. Burschka, *Angew. Chem.*, *Int. Ed. Engl.*, 1984, **23**, 806.
28 R. Rossi, A. Marchi, L. Marvelli, U. Castellato, S. Tamburini and R. Graziani, *J. Chem. Soc.*, *Dalton Trans.*, 1991, 263; R. Rossi, A. Marchi, L. Marvelli, L. Magor, M. Peruzzini, U. Castellato and R. Grazinai, *J. Chem. Soc.*, *Dalton Trans.*, 1993, 723.
29 A. Neher and I.-P. Lorenz, *Angew. Chem.*, *Int. Ed. Engl.*, 1989, **28**, 1342; G. B. Karet, C. L. Stern, D. M. Norton and D. F. Shriver, *J. Am. Chem. Soc.*, 1993, **115**, 9979; T. Chihara, T. Tase, H. Ogawa and Y. Wakatsuhi, *Chem. Commun.*, 1999, 279.
30 L. H. Vogt, Jr., L. J. Katz and S. E. Wiberley, *Inorg. Chem.*, 1965, **4**, 1157.
31 R. R. Ryan, G. J. Kubas, D. C. Moody and P. G. Eller, *Struct. Bonding* (*Berlin*), 1981, **46**, 47.
32 I. Ghatak, D. M. P. Mingos, M. B. Hursthouse and K. M. A. Malik, *Transition Met. Chem.*, 1979, **4**, 260.
33 K. A. Kubat-Martin, G. L. Kubas and R. R. Ryan, *Organometallics*, 1989, **8**, 910.
34 M. Meno, A. Pramanik, N. Bag and A. Chakravorty, *J. Chem. Soc.*, *Dalton Trans.*, 1995, 1543.
35 D. Sellmann, T. Gottschalk-Gaudig and F. W. Heinemann, *Inorg. Chim. Acta*, 1998, **209**, 63.
36 B. M. Mattson, J. R. Heiman and L. H. Pignolet, *Inorg. Chem.*, 1976, **15**, 564.
37 M. W. W. Adams, *Biochim. Biophys. Acta*, 1990, **1020**, 115; A. E. Pryzbyla, J. Robbins, N. Menon and H. D. Peck, *FEMS Microbiol. Rev.*, 1992, **88**, 109; R. K. Thauer, A. R. Klein and G. C. Hartmann, *Chem. Rev.*, 1996, **96**, 3031; J. W. Peters, W. N. Lanzilotta, B. J. Lemon and L. C. Seefeldt, *Science*, 1998, **282**, 1853.

Paper a907753g